第51卷第4期 中国科学技术大学学报 Vol. 51, No. 4
2021年4月 JOURNAL OF UNIVERSITY OF SCIENCE AND TECHNOLOGY OF CHINA Apr. 2021
Received: 2021-02-11; Revised: 2021-05-05 doi:10.52396/JUST-2021-0049

Development of the Ag nanoparticle-decorated Co_3O_4 electrode for high-performance hybrid Zn batteries

SHANG Wenxu, YU Wentao, MA Yanyi, TAN Peng*
Department of Thermal Science and Energy Engineering, University of Science and Technology of China, Hefei 230026, China
* Corresponding author. E-mail: pengtan@ustc.edu.cn

Abstract: The hybrid Zn battery is a promising electrochemical system integrating the redox reactions of transition metal oxides and oxygen in a single cell, through which high energy efficiency and energy density can be achieved simultaneously. However, the positive electrode usually suffers from unsatisfactory capacity utilization of the active material and poor oxygen reduction and evolution reaction activity. Here, a novel nano-structured Co_3O_4 electrode with the decoration of Ag nanoparticles is developed. Benefiting from the synergistic function between Ag nanoparticles and Co_3O_4 nanowires, the electric conductivity is improved and the morphology is optimized effectively. With this electrode, a hybrid Zn battery delivers five-step discharge voltage plateaus from 1.85 to 1.75, 1.6, 1.55, and 1.3 V, a high active material utilization ratio of 18%, and a low voltage gap of 0.69 V at 1 mA·cm^{-2}. Moreover, it can operate stably for 500 cycles with a voltage gap increase of only 0.03 V at 10 mA·cm^{-2}. This work brings up a novel electrode for an ultra-high performance hybrid Zn battery with both high active material utilization and outstanding oxygen electrocatalytic activity.
Keywords: hybrid Zn battery; cobalt oxide; Ag nanoparticles; active material utilization; voltage gap
CLC number: TQ152 **Document code**: A

1 Introduction

Zn-air batteries have attracted research attention due to their low cost, high theoretical energy density, and intrinsic safety[1-4]. However, restricted by the inferior oxygen reduction reaction (ORR) and oxygen evolution reaction (OER) catalytic activities, the high voltage gap causes unsatisfactory energy efficiency[5-7]. Although tremendous efforts concerning the ORR and OER catalysts have been conducted to address this issue, the theoretical potential (1.65 V) limits its further development[8-12].

Recently, a new type of hybrid Zn battery integrating Zn-M (M represents the transition metal or its oxide/hydroxide) and Zn-air battery is proposed, in which the high energy density and energy efficiency can be presented simultaneously[13-16]. During the discharge process, the reduction reaction of M occurs first and offers a discharge voltage of higher than 1.7 V, followed by the ORR to fully utilize the capacity of Zn; while during the charge process, the above reactions are reversed. Significantly, the positive electrode material can not only serve as the ORR and OER catalysts but also can serve as the active material of the redox reaction. Among them, Co oxides show superior performance due to their high theoretical capacity and excellent OER/ORR catalyst activity[17-20]. For example, Tan et al. developed a hybrid Zn battery with Co_3O_4 nanosheets electrodeposited on carbon cloth which delivered two discharge voltage plateaus: a high one of 1.85 V from the Zn-Co reaction and a low one of 1.0 V from the Zn-air reaction, effectively lifting the operating voltage[21]. Based on the oxygen vacancy-rich Co_3O_4, Liu et al. constructed a hybrid Zn battery with a high capacity of 790 mAh·g^{-1} and energy density of 928 Wh·kg^{-1}, and it can also work stably after 300 cycles[22].

For the hybrid Zn battery, the evaluation for the battery performance includes both the utilization of active material corresponding to the Zn-Co reaction region and the ORR/OER activity to the Zn-air reaction region. In a Zn-Co battery, the utilization ratio of active material can be improved through the microstructure modified or metal substitution. For example, Shang et al. reported a Co_3O_4 electrode with the heterogeneous porous nanowire, which shows a utilization ratio of 51.6%[23]. After substituted with Ni,

Citation: SHANG Wenxu, YU Wentao, MA Yanyi, et al. Development of the Ag nanoparticle-decorated Co_3O_4 electrode for high-performance hybrid Zn batteries. J. Univ. Sci. Tech. China, 2021, 51(4): 319-326.

the value can be further lifted to above 60%[24]. Even with these tremendous efforts, the intrinsic poor electric conductivity still limits its further improvement. When applied in the hybrid Zn battery, unfortunately, the utilization ratio is usually lower than 10% due to the addition of non-conductive binders, which hinders the contact between the active material and the electrolyte, therefore causing the ultralow utilization value[15]. On the other hand, although cobalt oxide is a bifunctional ORR/OER candidate catalyst, the ORR activity is insufficient, which also limits the performance of the Zn-air reaction region[25]. For instance, the discharge voltage is usually lower than 1.2 V even at a low current density of 1 mA · cm^{-2}[21]. Hence, the electrochemical performance for both two reaction regions should be further improved for the overall battery performance.

Ag is an excellent ORR catalyst with outstanding electric conductivity[26,27], and previous work has indicated that modification with Ag can dramatically improve the electric conductivity of pristine electrodes[28]. Huang et al. reported a composite of Ag nanoparticles and ZnO, in which the overlapping of electron accumulation region produces a percolation path. Consequently, the electron concentration is effectively increased, leading to a 1000-time increase in the electric conductivity[28]. Mao et al. fabricated a hybrid electrode made of $Ni(OH)_2$ grown on Ag nanowire, and the effective charge transfer between Ag and $Ni(OH)_2$ lifts the utilization of $Ni(OH)_2$ and avoids the useless zone, providing additional pseudocapacitance[29]. After assembled into a supercapacitor, the electrode demonstrates an optimal capacitance of 3103.5 F · g^{-1} and maintains 92.2% after 20000 cycles. Moreover, Ag particle has also been applied as the active material in a hybrid Zn battery, which exhibits high energy efficiency of 68% and operates stably after 100 cycles with almost no decay[26]. Nevertheless, RuO_2 must be added into the electrode to improve the OER activity, which lead to the extra cost and complexity during the synthesis process.

Herein, a novel Co_3O_4 electrode modified with Ag nanoparticles was fabricated for the hybrid Zn battery. Due to the addition of Ag, the utilization ratio of the Co_3O_4 electrode was improved, and the ORR activity is also improved effectively. With this structure design, the long high-discharge-voltage region and excellent OER/ORR catalytic activity can be achieved in a single cell, thus the overall battery performance can be ameliorated. To systematically study the Ag nanoparticle-decorated Co_3O_4 (Ag/Co_3O_4) electrode, the structure and morphology were characterized, and the multiple redox reactions were investigated. As for the battery behavior, the charge/discharge process under different current densities and the cycling stability were tested. This work paves a road of the electrode design for the high-performance hybrid Zn batteries.

2 Experimental

2.1 Fabrication of the Ag/Co_3O_4 electrode

The Co_3O_4 electrode was fabricated through a hydrothermal reaction as reported[23]. To obtain the Ag/Co_3O_4 electrode, 0.1 g of Ag powder with the size of 50 nm and 0.05 g of polytetrafluoroethylene (PTFE) with the size of 50 nm was mixed into 40 mL of water as precursor solution. Then the Co_3O_4 electrode was soaked in it for 1 min and dried at 60 ℃ with several times. After that, the prepared sample was heat-treated under 300 ℃ for 1 h in an N_2 atmosphere with a heating rate of 10 ℃ · min^{-1}. The loading of the sample was measured to be 2.22 mg · cm^{-2}. For comparison, the Co_3O_4 electrode was fabricated with a similar method without adding Ag powder, and the loading of the sample was measured to be 2.0 mg · cm^{-2}.

2.2 Material characterization

The material characterization was conducted at the Experimental Center of Engineering and Material Sciences in USTC. Detailedly, the X-ray powder diffraction (XRD, Smart lab) was conducted to investigate the spinel structure, the scanning electron microscope (SEM, XL-30 ESEM) was conducted to observe the morphologies and nanostructures.

2.3 Electrochemical measurement

The battery was assembled with the fabricated sample as the positive electrode, a zinc plate as the negative electrode, and 6 M KOH with 0.2 M $Zn(Ac)_2$ solution as the electrolyte. To investigate the electrochemical performance, the cycle voltammetry (CV) was conducted in an electrochemical workstation (Solartron Energy Lab) with the potential from 1.1 to 2.4 V (vs. Zn) using the scan rate from 1 to 20 mV · s^{-1}. The battery discharge and charge behaviors were tested at 1, 2, 5, and 10 mA · cm^{-2}, and the cycling performance was tested at 10 mA · cm^{-2} with 3 min discharge followed by 3 min charge. The utilization ratio of active material is calculated from the quotient of the practical specific discharge capacity (mAh · g^{-1}) and the theoretical capacity. In detail, the discharge areal capacity (mAh · cm^{-2}) is calculated through multiplying the applied current density and the corresponding discharge time of the Zn-M section, while the practical specific discharge capacity is calculated by the quotient of the practical areal discharge capacity and the mass loading (mg · cm^{-2}).

3 Results and discussion

3.1 Characterization of Ag/Co_3O_4 electrode

Figure 1 shows the XRD results from 20° to 80° of the Ag/Co_3O_4 electrode. Apart from the diffraction peaks of the nickel substrate, the other peaks can well assign to Co_3O_4 (PDF #42-1467) and Ag (PDF #04-0783), indicating the successful fabrication. The morphology of the sample was observed by SEM. As shown in Figure 2, the nanowires distributed uniformly on the surface of the Ni foam. From the high-magnification SEM images, the Ag nanoparticle can attach to the nanowires, which can greatly improve the contact surface with Co_3O_4, therefore lifting the electric conductivity of the electrode. To further confirm the addition of Ag nanoparticles in the electrode, the element mapping is illustrated in Figure 3. The metal of Ni, Co, O, Ag can be detected, which represent the Co_3O_4 and Ag on the Ni foam, manifesting the successful composition of Ag.

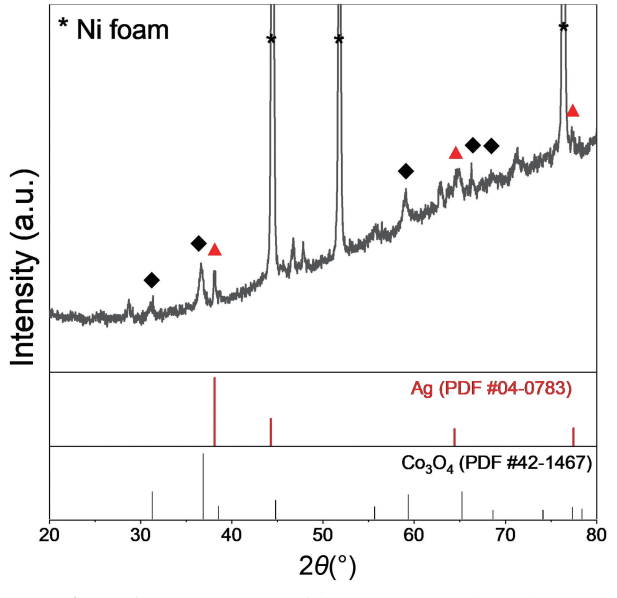

Figure 1. XRD pattern of the Ag/Co_3O_4 electrode.

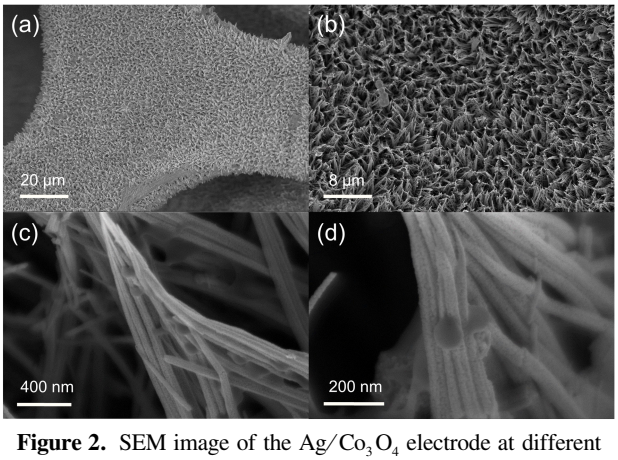

Figure 2. SEM image of the Ag/Co_3O_4 electrode at different magnifications: (a–b) overall microstructure coated on Ni foam; (c–d) distribution of Ag nanoparticles on nanowires.

3.2 Electrochemical performance of the Ag/Co_3O_4 electrode

The electrochemical performance of the Ag/Co_3O_4 electrode was first investigated in a two-electrode system. As shown in Figure 4, the CV curves were conducted from 1.1 to 2.4 V. Figure 4(a) displays four pairs of peaks, which represent $Ag \leftrightarrow Ag^+$ (Peaks 1 and 2), $Co^{2+} \leftrightarrow Co^{3+}$ (Peaks 3 and 4), $Co^{3+} \leftrightarrow Co^{4+}$ (Peaks 5 and 6), and $Ag^+ \leftrightarrow Ag^{2+}$ (Peaks 7 and 8), respectively. In contrast, the Co_3O_4 electrode only shows two pairs including the $Co^{2+} \leftrightarrow Co^{3+}$ and $Co^{3+} \leftrightarrow Co^{4+}$, indicating the existence of multiple reactions after the addition of Ag. Besides, the specific capacitance also increases from 873 to 1108 $F \cdot g^{-1}$ after the composite of Ag. Moreover, the signs from 1.1 to 1.4 and 2.2 to 2.4 represent the oxygen reduction reaction (ORR) and the oxygen evolution reaction (OER) section, respectively. Obviously, the Ag/Co_3O_4 electrode show much higher current densities in both ORR and OER sections than the Co_3O_4 electrode, demonstrating the improvement after the decoration of Ag nanoparticles. Figure 4(b) illustrates the CV curves of the Ag/Co_3O_4 electrode at different scan rates from 1 to 20 $mA \cdot cm^{-2}$. As the scan rate increases, the position of each peak change towards two sides gradually, which was caused by the increasing polarization. While the shape of CV curves can remain well and the peak can retain clearly, manifesting excellent stability.

To evaluate the discharge-capacity behaviors, a home-made battery was assembled. As shown in Figure 5(a), the battery displays five discharge voltage plateaus at 1 $mA \cdot cm^{-2}$: 1.85 V corresponds to $Ag^{2+} \rightarrow Ag^+$, 1.75 V for $Co^{4+} \rightarrow Co^{3+}$, 1.6 V for $Co^{3+} \rightarrow Co^{2+}$, 1.55 V for $Ag^+ \rightarrow Ag$, and 1.3 V for the ORR process, manifesting the multiple reactions. When operated under different current densities from 1 to 2, 5, and 10 $mA \cdot cm^{-2}$, the battery shows different discharge and charge voltages for Zn-air reaction of 1.30 V/1.99 V, 1.25 V/2.01 V, 1.16 V/2.05 V, and 1.10 V/2.07 V, respectively, and the corresponding voltage gap is 0.69, 0.76, 0.89, and 0.97 V, respectively (Figure 5(b)). Table 1 summarizes the discharge voltages of recent hybrid Zn batteries at 10 $mA \cdot cm^{-2}$, from which this battery shows four voltage plateaus from 1.8 to 1.6, 1.55, 1.1 V, more than the reported one. Significantly, the voltage during the Zn-air reaction is higher than others, such as $NiO/Ni(OH)_2$-CNT (1.08 V)[30], Co_3O_4 nanosheet (1.0 V)[21], Co_3O_4/carbon cloth (0.98 V)[31], and Ag-RuO_2/CNT (1.08 V)[26]. The optimal catalytic behavior in the Zn-air reaction can be attributed to the following reasons: ① the excellent

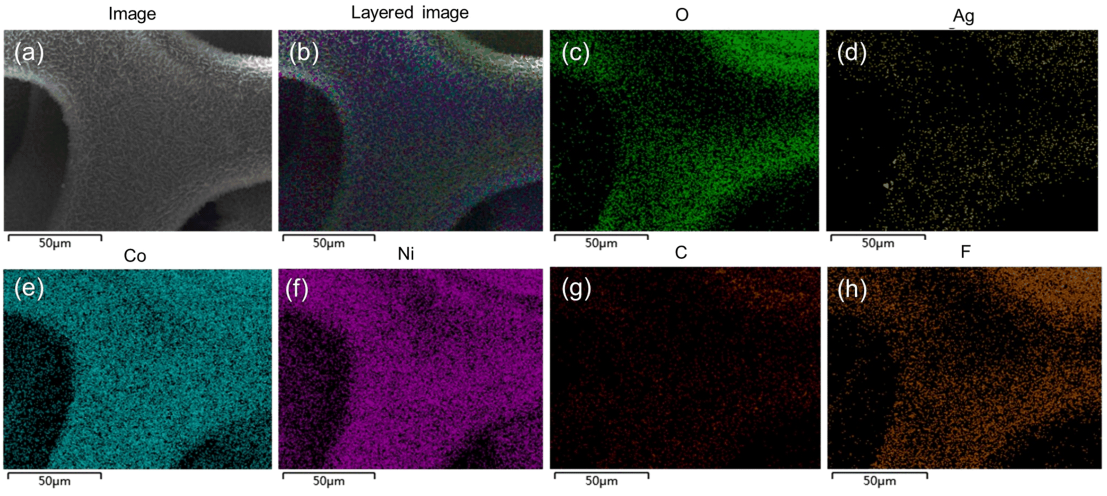

Figure 3. The elemental distribution of the Ag/Co_3O_4 electrode: (a) Pristine SEM image; (b) Layered image; (c–h) different elemental distribution images: (c) O, (d) Ag, (e) Co, (f) Ni, (g) C, and (h) F.

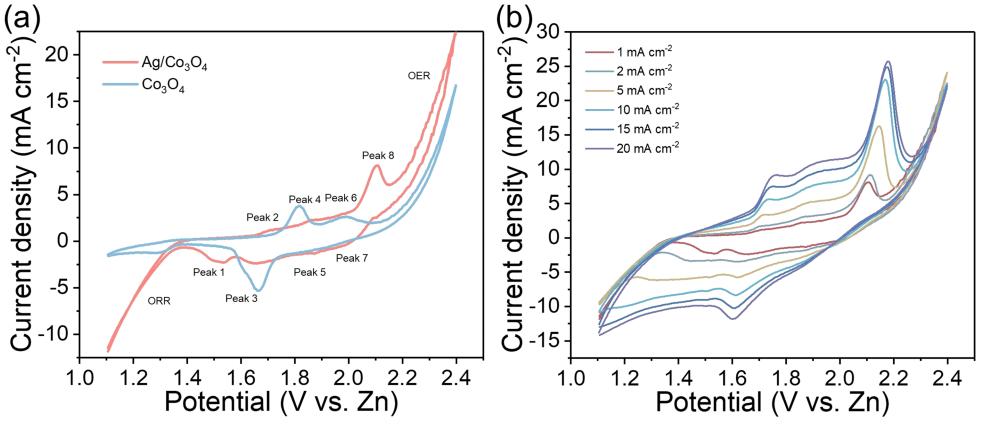

Figure 4. (a) Comparison of the CV curves between Co_3O_4 and Ag/Co_3O_4; (b) the CV curves of Ag/Co_3O_4 under different scan rates from 1 to 20 mA · cm^{-2}.

ORR activity of Ag particles can effectively reduce the overpotential of the electrode, leading to a high discharge voltage; ② the intrinsic good OER activity of Co_3O_4 can be also presented, reducing the charge voltage. As reported in the literature, to construct a hybrid Zn-Ag/air battery, RuO_2 is usually added due to the poor OER activity of Ag particles, which could increase the cost and complex the synthesis process[26]. Through modifying with Ag particles, the excellent ORR and OER activity can be achieved simultaneously with low cost, manifesting great market competitiveness. Besides, two parts of the battery performance are included for the hybrid battery: the utilization of active material in the Zn-M reaction and the discharge voltage in the Zn-air reaction. Therefore, the behavior of the Zn-M reaction should also be comprehensively considered to evaluate the battery performance. Figure 5 (c) compares the utilization ratios of active materials in recent reported hybrid batteries. Due to the poor reaction surface between the active material and the electrolyte, the utilization ratio is generally insufficient, which is even lower than 10%. This electrode displays the optimal utilization ratio of 18%, which is much higher than the other hybrid Zn-Co/air batteries, such as Co_3O_4/carbon cloth (6.5%)[31], Co_3O_4 nanosheets (6.7%)[21], coordination polymer derived oxygen vacancies rich Co_3O_4(7%)[32], $NiCo_2S_4$/3DNCC (11.2%)[33], oxygen vacancy-rich Co_3O_4 particles (12%)[22]. The great increase in the utilization ratio can be attributed to the following reasons: ① the decoration of Ag particles improve the conductivity of Co_3O_4 electrode, and therefore lifting the utilization ratio of active materials; ② the uniform distribution of Ag particles can effectively modify the electrode morphology, which is prone to the electron and ion transport.

To further investigate the electrochemical performance of the battery, the cycling behavior was

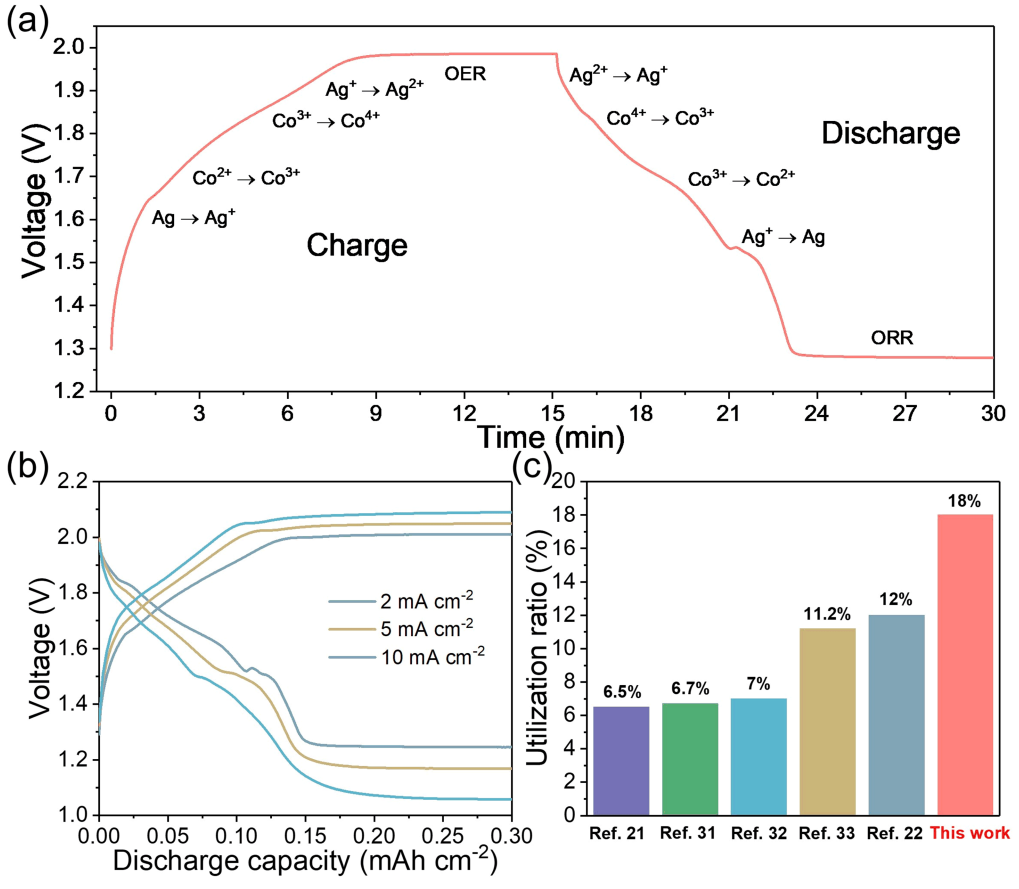

Figure 5. (a) Charge-discharge voltage curves at 1 mA · cm^{-2} with 15 min charge and 15 min discharge (The inset marks the corresponding reaction regions); (b) charge and discharge curves at different current densities from 2 to 10 mA · cm^{-2} of the hybrid Zn battery; (b) comparison of the utilization of active materials in the Zn-M reaction region.

tested under a current density of 10 mA · cm^{-2} with 3 min charge and 3 min discharge (Figure 6(a)). Initially, the battery shows a discharge voltage of 1.1 V and a charge voltage of 2.06 V with a potential gap of 0.96 V. During 500 cycles, the battery shows stable charge and discharge voltages. After the 500th cycle, the discharge and charge voltage is 1.08 and 2.07 V, respectively, and the voltage gap only increases to 0.99 V with an increase of only 30 mV, indicating excellent cycling stability. In comparison, the stability of Ag/Co_3O_4 composite is better than most reported electrodes in hybrid Zn batteries, such as Co_3O_4 nanosheets (200 cycles at 1 mA · cm^{-2})[21], Co_3O_4/carbon cloth (400 cycles at 10 mA · cm^{-2}, voltage gap increases 0.032 V)[31], oxygen vacancy-rich Co_3O_4 particles (300 cycles at 1 mA · cm^{-2})[22], $MnCo_2O_4$/nitrogen-doped reduced graphene oxide (100 cycles at 1 mA · cm^{-2})[34], NiO/Ni(OH)$_2$ nanoflakes (70 cycles at 1 mA · cm^{-2})[35], and NiO-Al-Co/Carbon cloth (192 cycles at 5 mA · cm^{-2})[30]. As for the Zn-M reaction region, it delivers the specific capacity of 0.21 mAh · cm^{-2} with a utilization ratio of 23.5%. After the 500th cycle, the capacity increases to 0.25 mAh · cm^{-2}, and the ratio lifts to 28%, which may be ascribed to the electrode activation during the cycle. Furthermore, the size of Ag nanoparticles also has a great effect on battery performances. When smaller Ag nanoparticles are applied, they can distribute more uniformly and the aggregation can be alleviated, leading to the larger specific surface area and electrochemical reaction area[36]. Therefore, both the active material utilization ratio and the catalytic activity can be improved. As for tuning the size of Ag nanoparticles, some effective strategies can be applied[37,38]. For instance, in the conventional hydrothermal reaction, the size decreases with an increase of the stabilizer during the reduction reaction (prevent the aggregation), decreases with an increase of the methanolic NaOH until an optimal amount, and decreases with the decline of water content[37]. Besides, some other reduction regents (e.g., $NaBH_4$) can also effectively decrease the size of Ag nanoparticles[38].

Table. 1. Performance comparison of hybrid Zn batteries based on different electrode materials.

Positive electrode materials	Performance			Ref.
	Discharge voltages (V) @10 mA · cm^{-2}	Cycling stability	Energy efficiency	
NiO/Ni(OH)$_2$ nanoflakes	1.7→1.1	70 cycles at 1 mA · cm^{-2} (70 min per cycle)	~80%	[35]
NiO/Ni(OH)$_2$-CNT	1.7→1.08	192 cycles at 5 mA · cm^{-2} (30 min per cycle)	>60%	[30]
Co_3O_4 nanosheet	1.85→1.0	200 cycles at 1 mA · cm^{-2} (30 min per cycle)	71%	[21]
Co_3O_4/Carbon cloth	1.7→0.98	400 cycles at 10 mA · cm^{-2} (4 min per cycle)	–	[31]
Ag + RuO_2/CNT	1.7→1.44→1.08	100 cycles at 4 mA · cm^{-2} (40 min per cycle)	~70%	[26]
Ag/Co_3O_4 composite	1.8→1.6→1.55→1.1	500 cycles at 10 mA · cm^{-2} (6 min per cycle)	~70%	This work

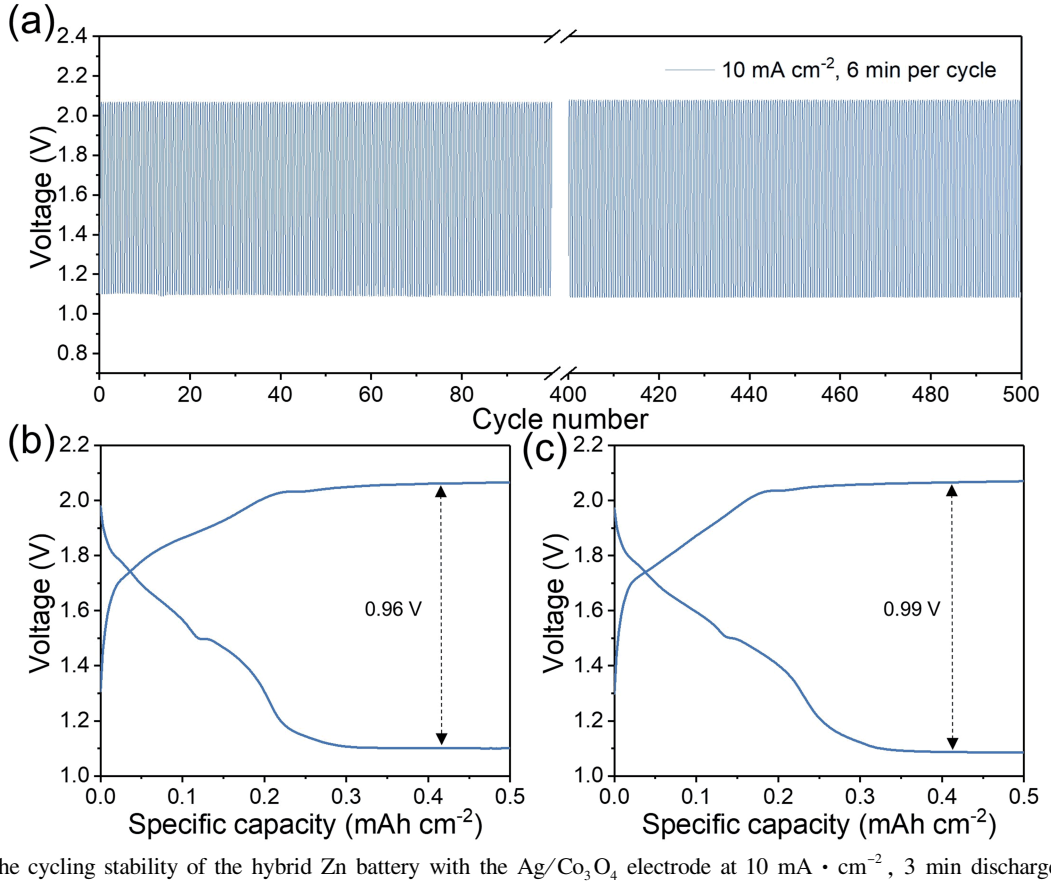

Figure 6. The cycling stability of the hybrid Zn battery with the Ag/Co_3O_4 electrode at 10 mA · cm^{-2}, 3 min discharge and 3 min charge: (a) the overall charge and discharge curves during 500 cycles; (b and c) the selected curves during the cycle: (b) the 1st and (c) the 500th cycle.

4 Conclusions

In summary, an Ag nanoparticle-decorated Co_3O_4 electrode was synthesized by mixing the Ag powder onto the surface of the Co_3O_4 electrode. Through the addition of Ag nanoparticles, the utilization ratio of active material and the ORR activity are improved simultaneously. With this electrode, a hybrid Zn battery shows five voltage plateaus of 1.85, 1.75, 1.6, 1.55, and 1.3 V at 1 mA · cm^{-2}, indicating the multiple voltage plateaus after the composition of Ag. Significantly, it delivers a high utilization ratio of 18% for the Zn-M reaction region. When operated under different current densities from 1 to 2, 5, 10 mA · cm^{-2}, the battery shows the small discharge and charge voltage gaps for the Zn-air reaction of 0.69, 0.76, 0.89, and 0.97 V, respectively. Besides, good cycling stability is also exhibited. After a 500 cycle test at 10 mA · cm^{-2}, the voltage gap only increases 0.03 V from 0.96 to 0.99 V. Hence, this work obtains an ultra-high

performance hybrid Zn-Co/air battery with both the high utilization ratio of active material and small voltage gap, indicating the potential application in the future.

Acknowledgments

This work is supported by Anhui Provincial Natural Science Foundation (2008085ME155), USTC Research Funds of the Double First-Class Initiative (YD2090002006), Joint Laboratory for USTC and Yanchang Petroleum (ES2090130110), and USTC Tang Scholar (KY2090000065).

Conflict of interest

The authors declare no conflict of interest.

Author information

SHANG Wenxu PhD candidate. Research field: Electrochemical energy storage systems.

YU Wentao PhD candidate. Research field: zinc electrode and zinc-air flow batteries.

MA Yanyi PhD candidate. Research field: electrode materials of hybrid Zn-air batteries.

TAN Peng Corresponding author, Professor. Research field: Advanced energy storage systems.

References

[1] Parker J F, Chervin C N, Pala I R, et al. Rechargeable nickel-3D zinc batteries: An energy-dense, safer alternative to lithium-ion. Science, 2017, 356(6336): 415-418.

[2] Fu J, Cano Z P, Park M G, et al. Electrically rechargeable zinc-air batteries: Progress, challenges, and perspectives. Advanced Materials, 2017, 29(7): 1604685.

[3] Tan P, Chen B, Xu H R, et al. Flexible Zn- and Li-air batteries: Recent advances, challenges, and future perspectives. Energy and Environmental Science, 2017, 10(10): 2056-2080.

[4] Zhu X F, Hu C G, Amal R, et al. Heteroatom-doped carbon catalysts for zinc-air batteries: Progress, mechanism, and opportunities. Energy & Environmental Science, 2020, 13(12): 4536-4563.

[5] Tan P, Chen B, Xu H R, et al. Synthesis of Fe_2O_3 nanoparticle-decorated *n*-doped reduced graphene oxide as an effective catalyst for Zn-air batteries. Journal of the Electrochemical Society, 2019, 166(4): A616-A622.

[6] Fu J, Liang R L, Liu G H, et al. Recent progress in electrically rechargeable zinc-air batteries. Advanced Materials, 2018, 29(7): 1805230.

[7] Wang F, Zhang B, Zhang M Y, et al. A rechargeable zinc-air battery based on zinc peroxide chemistry. Science, 2021, 371(6524): 46-51.

[8] Tan Y Y, Zhang Z Y, Lei Z, et al. Thiourea-zeolitic imidazolate framework-67 assembly derived Co-CoO nanoparticles encapsulated in N, S codoped open carbon shell as bifunctional oxygen electrocatalyst for rechargeable flexible solid Zn-air batteries. Journal of Power Sources, 2020, 473: 228570,

[9] Liu X Z, Tang T, Jiang W J, et al. Fe-doped Co_3O_4 polycrystalline nanosheets as binder-free bifunctional cathode for robust and efficient zinc-air batteries. Chemical Communications, 2020, 56(40): 5374-5377.

[10] Xie S L, Lin J J, Wang S S, et al. Rational design of hybrid Fe_7S_8/Fe_2N nanoparticles as effective and durable bifunctional electrocatalysts for rechargeable zinc-air batteries. Journal of Power Sources, 2020, 457: 228038.

[11] Guo Y B, Yao S, Gao L X, et al. Boosting bifunctional electrocatalytic activity in S and N co-doped carbon nanosheets for high-efficiency Zn-air batteries. Journal of Materials Chemistry A, 2020, 8(8): 4386-4395.

[12] Li S M, Yang X H, Yang S Y, et al. An amorphous trimetallic (Ni-Co-Fe) hydroxide-sheathed 3D bifunctional electrode for superior oxygen evolution and high-performance cable-type flexible zinc-air batteries. Journal of Materials Chemistry A, 2020, 8(11): 5601-5611.

[13] Tan P, Chen B, Xu H R, et al. In-situ growth of Co_3O_4 nanowire-assembled clusters on nickel foam for aqueous rechargeable Zn-Co_3O_4 and Zn-air batteries. Applied Catalysis B: Environmental, 2019, 241: 104-112.

[14] Zhong Y T, Xu X M, Liu P Y, et al. A function-separated design of electrode for realizing high-performance hybrid zinc battery. Advanced Energy Materials, 2020, 10: 2002992.

[15] Shang W X, Yu W T, Tan P, et al. Achieving high energy density and efficiency through integration: Progress in hybrid zinc batteries. Journal of Materials Chemistry A, 2019, 7(26): 15564-15574.

[16] Tan P, Chen B, Xu H R, et al. Growth of Al and Co co-doped NiO nanosheets on carbon cloth as the air electrode for Zn-air batteries with high cycling stability. Electrochimica Acta, 2018, 290: 21-29,

[17] Ma Y Y, Xiao X, Yu W T, et al. Mathematical modeling and numerical analysis of the discharge process of an alkaline zinc-cobalt battery. Journal of Energy Storage, 2020, 30: 101432,

[18] He D, Song X Y, Li W Q, et al. Active electron density modulation of Co_3O_4 based catalysts endows highly oxygen evolution capability. Angewandte Chemie., International Edition, 2020, 59(17): 2-9,

[19] Lu Y Z, Wang J, Zeng S Q, et al. An ultrathin defect-rich Co_3O_4 nanosheet cathode for high-energy and durable aqueous zinc ion batteries. Journal of Materials Chemistry A, 2019, 7(38): 21678.

[20] Xiao X, Hu X Y, Liang Y, et al. Anchoring $NiCo_2O_4$ nanowhiskers in biomass-derived porous carbon as superior oxygen electrocatalyst for rechargeable Zn-air battery. Journal of Power Sources, 2020, 476: 228684.

[21] Tan P, Chen B, Xu H R, et al. Co_3O_4 nanosheets as active material for hybrid Zn batteries. Small, 2018, 14(21): 1800225.

[22] Liu N, Hu H L, Xu X X, et al. Hybrid battery integrated by Zn-air and Zn-Co_3O_4 batteries at cell level. Journal of Energy Chemistry, 2020, 49(10): 375-383.

[23] Shang W X, Yu W T, Xiao X, et al. Microstructure-tuned cobalt oxide electrodes for high-performance Zn-Co batteries. Electrochimica Acta, 2020, 353: 136535.

[24] Shang W X, Yu W T, Xiao X, et al. Unravel the influences of Ni substitution on Co-based electrodes for rechargeable alkaline Zn-Co batteries. Journal of Power Sources, 2021, 483: 229192.

[25] Tan P, Wu Z, Chen B, et al. Exploring oxygen electrocatalytic activity and pseudocapacitive behavior of Co_3O_4 nanoplates in alkaline solutions. Electrochimica Acta, 2019, 310: 86-95.
[26] Tan P, Chen B, Xu H R, et al. Integration of Zn-Ag and Zn-air Batteries: A hybrid battery with the advantages of both. ACS Applied Materials and Interfaces, 2018, 10(43): 36873-36881.
[27] Yuksel R, Alpugan E, Unalan H E. Coaxial silver nanowire/polypyrrole nanocomposite supercapacitors. Organic Electronics, 2018, 52: 272-280.
[28] Huang P S, Qin F, Lee J K. Role of the interface between Ag and ZnO in the electric conductivity of Ag nanoparticle-embedded ZnO. ACS Applied Materials and Interfaces, 2020, 12(4): 4715-4721.
[29] Mao Y Y, Xie J Y, Liu H, et al. Hierarchical core-shell Ag@Ni(OH)$_2$@PPy nanowire electrode for ultrahigh energy density asymmetric supercapacitor. Chemical Engineering Journal, 2020, 405: 126984.
[30] Tan P, Chen B, Xu H R, et al. Nanoporous NiO/Ni(OH)$_2$ Plates Incorporated with carbon nanotubes as active materials of rechargeable hybrid zinc batteries for improved energy efficiency and high-rate capability. Journal of The Electrochemical Society, 2018, 165(10): A2119-A2126.
[31] Tan P, Chen B, Xu H R, et al. Investigation on the electrode design of hybrid Zn-Co_3O_4/air batteries for performance improvements. Electrochimica Acta, 2018, 283: 1028-1036.
[32] Xu D D, Wu S T, Xu X X, et al. Hybrid Zn battery with coordination-polymer-derived, oxygen-vacancy-rich Co_3O_4 as a cathode material. ACS Sustainable Chemistry & Engineering, 2020, 8(11): 4384-4391.
[33] Wang X X, Xu X X, Chen J, et al. Combination of Zn-$NiCo_2S_4$ and Zn-air batteries at the cell level: A hybrid battery makes the best of both worlds. ACS Sustainable Chemistry and Engineering, 2019, 7(14): 12331-12339.
[34] Qaseem A, Chen F Y, Qiu C Z, et al. Reduced graphene oxide decorated with manganese cobalt oxide as multifunctional material for mechanically rechargeable and hybrid zinc-air batteries. Particle and Particle Systems Characterization, 2017, 34(10): 1-14.
[35] Lee D U, Fu J, Park M G, et al. Self-assembled NiO/Ni(OH)$_2$ nanoflakes as active material for high-power and high-energy hybrid rechargeable battery. Nano Letters, 2016, 16(3): 1794-1802.
[36] Lee K C, Lin S J, Lin C H, et al. Size effect of Ag nanoparticles on surface plasmon resonance. Surface and Coatings Technology, 2008, 202(22-23): 5339-5342.
[37] He B, Tan J J, Liew K Y, et al. Synthesis of size controlled Ag nanoparticles. Journal of Molecular Catalysis A: Chemical, 2004, 221(1-2): 121-126.
[38] Agnihotri S, Mukherji S, Mukherji S. Size-controlled silver nanoparticles synthesized over the range 5-100 nm using the same protocol and their antibacterial efficacy. RSC Advances, 2014, 4(8): 3974-3983.

构建银纳米颗粒修饰的四氧化三钴电极用于高性能复合锌电池

尚文旭,俞文涛,马彦义,谈鹏*
中国科学技术大学热科学和能源工程系,安徽合肥 230026
*通讯作者. E-mail: pengtan@ustc.edu.cn

摘要: 复合锌电池将过渡金属氧化物和氧气的氧化还原反应整合到一个电池中,可以同时实现高能量效率和高能量密度,是一种极具发展前景的电化学系统. 然而,正极通常面临活性物质容量利用率低以及氧还原和析出反应活性差的问题. 通过构建一种新型具有银纳米粒子修饰的四氧化三钴电极,得益于银纳米颗粒与四氧化三钴纳米线之间的协同作用,导电性得到了改善,形貌得到了有效的优化. 使用该电极,复合锌电池可实现在1.85至1.75、1.6、1.55和1.3 V的电压范围内五级平稳放电,在1 mA·cm^{-2}时具有18%的高活性材料利用率和0.69 V的低电压差;而且,可以稳定运行500个充放电循环,在10 mA·cm^{-2}时电压差仅增加0.03 V. 这为超高性能复合锌电池提供了一种兼具高活性材料利用率和高氧电催化活性的新型电极.

关键词: 复合锌电池;氧化钴;银纳米颗粒;活性物质利用率;电压差